nucleus to the sinus wall (*2*). The cell then has to pass through the sinus wall in order to enter the circulation.

Our materials were obtained from 12 New Zealand white rabbits, 1 to 8 weeks old. With the animals under general anesthesia, the marrow tissue was removed from tibia and femur after splitting the bones. The tissue was immediately immersed in Karnovsky's glutaraldehyde-formaldehyde mixture buffered in sodium cacodylate, where it was fixed for 24 hours. After it was rinsed in the buffer, the tissue was fixed in 2 percent OsO_4 similarly buffered. It was then dehydrated, embedded in Araldite, sectioned in an LKB microtome with a diamond knife, and studied in a Hitachi HU 11-A microscope.

The endothelial cell of the sinus wall had an elongated nucleus. Its cytoplasm was stretched to make up the bulk of the sinus wall, which was very thin and at times extremely attenuated. When the cytoplasms of two endothelial cells came into contact, they were held by junctional complexes, usually of the zonula adherens type. No gaps were present in these junctions, a feature distinguishing these sinuses from lymphatics (*3*). No passage of red cells through these junctions was observed. Passage occurred through pores of various sizes (1 to 4 μm) at irregular intervals in the endothelial cytoplasm of the sinus wall (Fig. 1).

The continuity of the cytoplasm in the area below the pore was shown in serial sections, which indicated that these pores are within the cytoplasm of a single cell and are not gaps at the juncture of two endothelial cells. The pore size appeared relatively fixed, exerting a control on the passing cells, which must conform to this size in order to traverse the wall. The cytoplasm of the passing cells was seen to squeeze through these pores (Fig. 1A), and the cytoplasmic organelles, such as mitochondria and ribosomes, and small nuclear fragments (Howell-Jolly bodies) were small enough to conform to the pore size. They were also seen in passage through the apertures. The rigid nucleus of the red cell, however, could not conform to the pore size. When nucleated red cells were seen in passage, the nucleus was caught and the cell became enucleated (Fig. 1B). In this manner, the red cell less its nucleus entered the circulation as a blood reticulocyte and the nucleus remained in the hematopoietic compartment of the marrow (Fig. 1C) where it was ingested by macrophages (Fig. 1D).

The morphological basis of this pit ting function in the endothelium of marrow sinuses is not immediately clear. Even in high-resolution microscopy, no specialized grommet-like structure was seen in the portion of endothelium adjacent to the pore. This is of interest because in the endothelium of splenic sinuses, bands of microfilaments determine the pore size and thereby control transmural cellular passage (*4*). In our materials, bands of microfilaments were present in the endothelium of marrow sinuses. These structures, however, were located beneath the cytoplasmic membrane in the abluminal side. We did not observe bands of microfilaments in the areas adjacent to the grommets. In the spleen, the pores are potential and the passing cell must find its way between two endothelial cells normally in juxtaposition. During the passage, the pore size is controlled by bands of microfilaments that prevent the endothelial cells from being forced too far apart. In marrow, however, the pores are actual and the passage of erythrocytes is transcellular

MEHDI TAVASSOLI
WILLIAM H. CROSBY
L. C Jacobson Blood Center, Scripps Clinic and Research Foundation, La Jolla, California 92037

References and Notes

1. W. H. Crosby, *Blood* **12**, 165 (1957); *ibid.* **14**, 399 (1959); S. Koyama, S. Aoki, K. Deguchi, *Mie Med. J.* **14**, 143 (1964); R. A. Rifkind, *Blood* **26**, 433 (1965); N. S. Lawson, B. Schnitzer, E. B. Smith, *Arch. Pathol.* **87**, 501 (1969).
2. J. A. Grasso, H. Swift, G. A. Ackerman, *J Cell Biol.* **14**, 235 (1962); L. Weiss, *J. Morphol.* **117**, 467 (1965); D. Orlic, A. S. Gordon, J. Rhodin, *J. Ultrastruct. Res.* **13**, 516 (1965); C. F Simpson and J. M. Kling, *J. Cell Biol* **35**, 237 (1967); E. Skutelsky and D. Danon, *ibid.* **33**, 634 (1967); F. R. Campbell, *Anat Rec.* **160**, 539 (1968); *Amer. J. Anat.* **135**, 521 (1972).
3. L. V. Leak, *Microvasc. Res.* **2**, 361 (1970).
4. L. T Chen and L. Weiss, *Amer. J Anat.* **134** 425 (1972).
5. Supported by NIH grant AM-16501-01 and AEC contract AT(11-1)3375.

20 November 1972; revised 2 January 1973

Proton Beam Radiography in Tumor Detection

Abstract. *Monoenergetic protons are highly sensitive to density variations and are capable of giving radiographs of very high contrast. As an initial step in exploring their diagnostic potential, protons with energies of 160 million electron volts are used in "contact radiography" on tumor-bearing human brain specimens. The proton radiographs are compared with x-radiographs taken under identical specimen conditions.*

Unlike x-ray and neutron fluxes, which are attenuated in an exponential relationship with absorber thickness, the proton flux shows only moderate attenu ation before dropping off very steeply at the end of the particle range. This property may be used to advantage fo by placing a photographic film in the region of the steepest part of the flux-depth curve radiographs of unusually high contrast may be obtained (*1*). Furthermore, radiography based on transmission of protons is relatively insensitive to variations in chemical com-

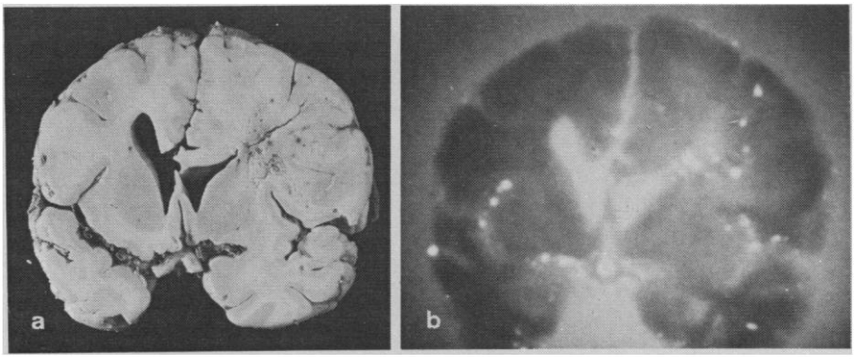

Fig. 1. (a) Front view of a coronal slice 1 cm thick of a human brain fixed in formalin. Note the glioblastoma multiforme in the white matter of the hemisphere on the right, with swelling of the hemisphere and distortion of the ventricular system. (b) Proton radiograph. Note the decreased density in the tumor area and the visualization of the basal ganglia. The white spots are air bubbles. The conditions were 115-cm focus to film, no screen, Polaroid TLX film, and a dose to the first surface of approximately 290 rad in 0.8 minute.

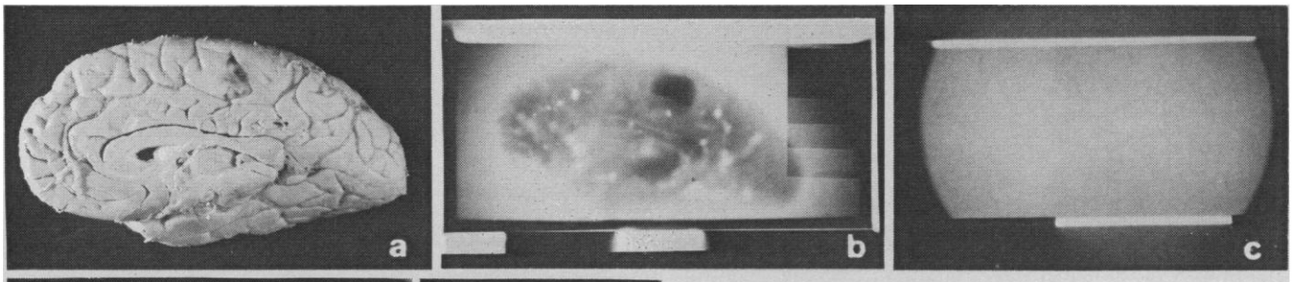

Fig. 2. (a) Medial view of formalin-fixed right hemisphere, showing a metastasis from a mucin-producing adenocarcinoma of the pancreas below the midpoint of the superior border. (b) Proton radiograph of the hemisphere. The conditions were 115-cm focus to film, no screen, Polaroid TLX film, and a dose to the first surface of approximately 290 rad in 0.8 minute. (c) X-radiograph of the hemisphere in a plastic water box. The conditions were 126-cm focus to film, Dupont high-speed 1A screen, Polaroid TLX film in Polaroid cassette, 30-kv peak, 200 ma, 3.0 seconds. (d) X-radiograph of the hemisphere in air. The specimen was reconstructed from serial coronal sections. Note that the tumor is just visible. The conditions (optimal) were 92-cm focus to Kodak mammography film, 27-kv constant potential, 20 ma, 2 minutes. (e) Photograph of a slice taken through the tumor.

position within the absorber but, in comparison, is highly sensitive to density variations. These properties have been used for the visualization of density variations within human pathologic tissue specimens as a first stage in a program to determine the usefulness of this method as a diagnostic tool.

We have employed the external beam of 160-Mev protons from the Harvard cyclotron. The beam transport system delivers a focused beam 0.5 cm in diameter. In order that a broad beam of good uniformity may illuminate the specimen, the beam is diffused by transmission through a target of lead or copper. The proton energy is consequently reduced, typically to 137 Mev, but at a distance of 3 m the proton flux is nearly uniform to a radius of 10 cm from the beam line. It is within this region that the specimen is placed. Immediately downstream of the specimen a photographic film is positioned for the exposure. This technique may appropriately be called "contact radiography" because it resembles the method for making contact prints of a negative.

Several types of photographic film have been tested to explore picture quality and sensitivity. For the work reported here we used Polaroid TLX radiographic film packets because of their great convenience. In order to neutralize approximately the effects of irregularity of shape of the specimen, and thus show primarily the effect of tissue-density variations, we immersed the entire specimen in water contained in a plastic box with parallel faces. The energy of the protons incident on the box was adjusted by adding thin polystyrene absorbers to the scattering target until radiographs of optimum contrast were obtained. On the basis of images of step wedges, we find that steps of 0.01 g/cm^2 can be distinguished.

Figure 1 illustrates the results obtained on a coronal slice 1 cm thick taken through a human brain with a primary neuroectodermal tumor (glioblastoma multiforme) located within the left hemisphere. Figure 2 shows the results obtained for a metastatic tumor from the pancreas and, for comparison, optimal x-radiographs of the specimen. In the investigation reported here prepared specimens were used, so that no effort was made to reduce the radiation dose required for an exposure. In a separate investigation we have found that satisfactory pictures can be obtained by using intensifying screens at dose levels to the first surface of less than 1 rad.

Under identical specimen conditions the proton beam method offers a better means of visualization of the internal structure and the tumors contained in a specimen than does the x-ray technique. Furthermore, it is possible to note distortions of the cerebral outline because there is sufficient density variation between the immersion fluid and the specimen.

To our knowledge, no previous publication has demonstrated proton radiography of human tissues nor the contrast obtainable by this technique between several normal and malignant tissues. Proton images of a living rat have been attempted (*2*), and the stopping power of protons in human skull-bone has been measured (*3*). Microradiography of tissue sections with alpha particles from ^{210}Po has also shown useful contrast between several tissues (*4*). We have used the proton radiographic technique for the detection and delineation of other cerebral tumors, and for tumors elsewhere in the body, such as carcinoma of the breast (*5*). A scintillator-television dynamic approach has been shown to be useful (*6*).

V. W. STEWARD
Neuropathology Laboratory,
University of Chicago,
Chicago, Illinois 60637

A. M. KOEHLER
Cyclotron Laboratory,
Harvard University,
Cambridge, Massachusetts 02115

References and Notes

1. A. M. Koehler, *Science* **160**, 303 (1968).
2. B. Jung, "On the application of 185 MeV protons in radiograpny and densitometry" (Report GWI-RZ/68, Gustaf Werner Institute, Uppsala, Sweden, 1968).
3. A. M. Koehler, J. G. Dickinson, W. M. Preston, *Radiat. Res.* **26**, 334 (1965).
4. L. F. Belanger and C. Belanger, *J. Biophys. Biochem. Cytol.* **6**, 197 (1959).
5. V. W. Steward and A. M. Koehler, in preparation.
6. H. Berger, N. P. Lapinski, N. S. Beyer, in *Proceedings of the 8th Symposium on Nondestructive Evaluation in Aerospace, Weapons Systems, Nuclear Applications* (Southwest Research Institute, San Antonio, Texas, 1971) pp. 102–111.
7. The generous contribution of film and the loan of equipment by the Polaroid Corporation, Cambridge, Massachusetts, is gratefully acknowledged. Supported in part by NSF grant GI 32991X and an institutional grant from the American Cancer Society (IN-41L. 5035).

10 July 1972; revised 10 October 1972